DOI: 10.1002/ejoc.201500647

Ferrocenoyl-Substituted Pyrimidine Nucleobases: An Experimental and Computational Study of Regioselective Acylation of Uracil, Thymine, and 5-Fluorouracil

Jasmina Lapić,[a] Valentina Havaić,[b] Davor Šakić,[b] Krešimir Sanković,[b] Senka Djaković,*[a] and Valerije Vrček*[b]

Keywords: Reaction mechanisms / Density functional calculations / Acylation / Regioselectivity / Nucleobases

Uracil, thymine, and 5-fluorouracil (5-FU) have been ferrocenoylated selectively at the N^1 position. Deprotonated pyrimidine nucleobases, prepared with sodium hydride (NaH) in *N*,*N*-dimethylformamide (DMF), reacted with either ferrocenoyl chloride (FcCOCl) or ferrocenoyl ethyl carbonate (FcCOOCOOEt), in DMF to give a single product. The regioselectivity of these reactions were analyzed in detail by using NMR spectroscopy and quantum chemical calculations. The ^{1}H and ^{19}F NMR spectra of reaction mixtures, and ^{13}C NMR and 2D NOESY spectra of products, confirmed the formation of the N^1-isomer only. The calculated energy barrier for acetylation at the N^3-position is significantly higher (> 40 kJ/mol), which suggests that the analogous reaction at the N^1-position is kinetically controlled. The nucleophilic addition of pyrimidine bases to the carbonyl group of FcCOCl proceeds through a concerted S_N2-like mechanism with the absence of the generally assumed tetrahedral intermediate.

Introduction

The ferrocenyl fragment has been coupled to a plethora of biologically relevant systems, such as peptides, sugars, drugs, and nucleosides.[1] In this respect, nucleobases remain attractive targets for ferrocenyl conjugation. Pyrimidines and purines substituted by a ferrocenyl moiety present interesting organometallic conjugates because their structures incorporate both biologically and electrochemically active components.[2] A series of ferrocene-substituted nucleobases has been described incorporating a different set of linkers, but no carbonyl group has been used as a chemical spacer. Carbonyl spacers enable extended conjugation involving ferrocenyl and nucleobase aromatic moieties, and the electron delocalization can be tuned by inserting substituents at the ferrocene ring system.

In this work, the Fc–C=O fragment has been linked to "standard" pyrimidine bases uracil and thymine. In addition, the ferrocenyl moiety is attached to 5-fluorouracil (5-FU), which is a nucleobase analogue of known pharmacological significance.[3] It is expected that the ferrocenyl group can modulate or potentiate the biological activity of the conjugated pharmacophores.

To replace the sugar part of pyrimidine nucleosides with a ferrocene moiety, the parent nucleobases should be substituted selectively at the N^1-position. In this report, synthetic procedures for the preparation of N^1-ferrocenoyl-substituted pyrimidine bases (thymine, uracil, and 5-FU) have been developed. No protection of the N^3-position is needed to afford the N^1-isomer as a single product. The regioselective N^1-substitution was confirmed by NMR spectroscopic analysis, and quantum chemical calculations were performed to rationalize the kinetic preference for the N^1-acylation reaction.

Results and Discussion

To prepare N^1-ferrocenoyl-substituted uracil, thymine, or 5-fluorouracil, several bases (K_2CO_3, TEA, or NaH) were probed as deprotonating agents for pyrimidines. Attempts at the preparation with K_2CO_3 or TEA were less effective in terms of both yield and efficacy. By using NaH as a deprotonating agent, exclusive formation of the N^1-isomer in high yield was observed. The acidity of N^1 and N^3 protons in uracil (or thymine) is essentially identical in solution,[4–6] and therefore cannot account for the observed regioselectivity. Herewith, we employ NMR spectroscopy and quantum chemical methods to rationalize the mechanism underlying the regioselectivity of the reaction between deprotonated nucleobases and FcCOCl (or FcCOOCOOEt) (Scheme 1).

[a] Faculty of Food Technology and Biotechnology, University of Zagreb,
Pierottijeva 6, Zagreb, Croatia
E-mail: sdjakov@pbf.hr
http://www.pbf.unizg.hr/en/departments/department_of_chemistry_and_biochemistry/laboratory_for_organic_chemistry/senka_djakovic
[b] Faculty of Pharmacy and Biochemistry, University of Zagreb, Ante Kovačića 1, Zagreb, Croatia
E-mail: vvrcek@pharma.hr
http://www.pharma.unizg.hr/en/about-us/staff/valerije-vrcek,391.html

Supporting information for this article is available on the WWW under http://dx.doi.org/10.1002/ejoc.201500647.

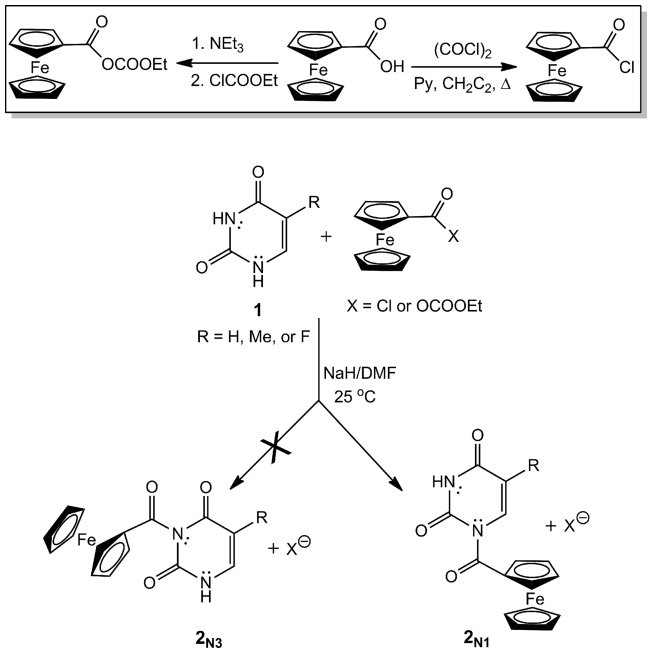

Scheme 1. Regioselective N^1-acylation of pyrimidine nucleobases **1** (uracil, R = H; thymine, R = Me; 5-fluorouracil, R = F) with ferrocenoyl chloride (X = Cl) or ferrocenoyl ethyl carbonate (X = $OCOOCH_2CH_3$). Preparation of ferrocenoyl chloride (FcCOCl) and ferrocenoyl ethyl carbonate (FcCOOCOOEt) from ferrocenecarboxylic acid (FcCOOH) is presented in the inset box.

The Reaction Mechanism

To investigate the mechanism of the reaction between pyrimidine bases and FcCOCl, DFT calculations were performed. Stationary points were searched at the corresponding potential energy surfaces, and characterized as either minima (NImag = 0) or first-order saddle points (NImag = 1). For the reaction between N^1-deprotonated uracil (**1_{N1}**, R = H) and FcCOCl, only one transition state (**TS_{N1}**) was located (Figure 1). This transition structure connects reactants (**1_{N1}** and FcCOCl) and the product (**2_{N1}**, R = H), as

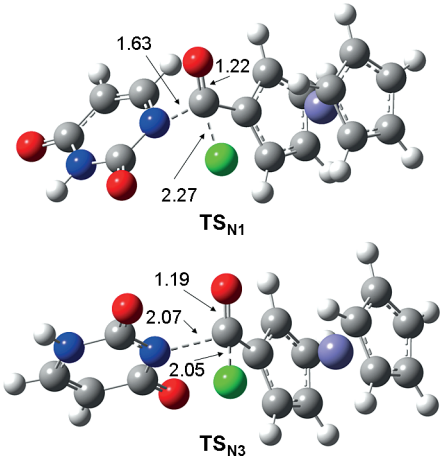

Figure 1. Transition-state structures **TS_{N1}** and **TS_{N3}** for the reaction of N^1- or N^3-deprotonated uracil, respectively, with ferrocenoyl chloride (FcCOCl), optimized at the B3LYP/6-31G(d) level. All distances are in angstroms.

followed by the IRC procedure, which suggests a concerted S_N2-type mechanism.

The same mechanism is operative for the reaction between N^3-deprotonated uracil (**1_{N3}**, R = H) and FcCOCl, in which a single transition state (**TS_{N3}**) exists on the corresponding energy surface. No tetrahedral intermediate, typical of a nucleophilic addition–elimination mechanism, was found in either case. All starting structures of conceivable intermediates converged, during geometry optimization, to local minima at the reactant or product side of the reaction. Therefore, the reaction between uracil and FcCOCl follows a one-step mechanism in which N–C bond formation and C–Cl bond cleavage occur simultaneously. This supports earlier theoretical and experimental results that corroborate that nucleophilic addition to the carbonyl group of acid chlorides proceeds by a concerted S_N2-like mechanism with the absence of the generally assumed tetrahedral intermediate.[7–9]

The one-step mechanism is operative in the reaction between other pyrimidine bases, thymine (**1_{N1}**, R = Me) or 5-fluorouracil (**1_{N1}**, R = F), and FcCOCl, as evidenced by our computational results. However, if a poor leaving group is incorporated in the acylating agent, then the "classical" two-step mechanism becomes operative. According to the computational results, in the reaction between neutral uracil and ferrocenoyl ester ($FcCOOCH_3$) and ferrocenecarboxylic acid (FcCOOH), the tetrahedral intermediate was easily located in both cases (see Figure S1 in the Supporting Information). This finding reveals the stepwise mechanism for nucleophilic substitution at the carbonyl carbon. Again, this is in agreement with experimental evidence of an addition–elimination pathway, which is a preferred reaction channel when the acylating agent contains poor leaving groups.[10]

Regioselectivity of the Acylation Reaction

In the following section, we will investigate the regioselectivity of the reaction between pyrimidine bases and FcCOCl. Reports on regioselective acylations of uracil and thymine are rather scarce.[11,12] Most of the reactions between unprotected uracil/thymine derivatives and acylating agents (acylchlorides, esters, or anhydrides) result in the formation of a mixture of N^1- and N^3-substituted products.[13] It has been found that the N-acylation position depends on the reaction temperature, base, catalyst, and acylation agent employed.[14,15]

In case of the reaction between thymine and FcCOCl, only one product was observed spectroscopically (Figure 2). The reaction was followed by the sampling method in which aliquots (0.2 mL) were taken directly from the reaction mixture at selected time points. The ^1H NMR spectrum of each aliquot was measured in [D_6]DMSO. Along with the disappearance of signals of the reactant (the ring protons for FcCOCl in the range of 4–5 ppm), a new set of proton signals of the product emerged (Figure 3). According to detailed ^1H, ^{13}C, and 2D NOESY NMR analysis of the prod-

uct obtained (see below), we conclude that a N^1-ferrocenoyl conjugate ($\mathbf{2_{N1}}$, R = Me) was formed.

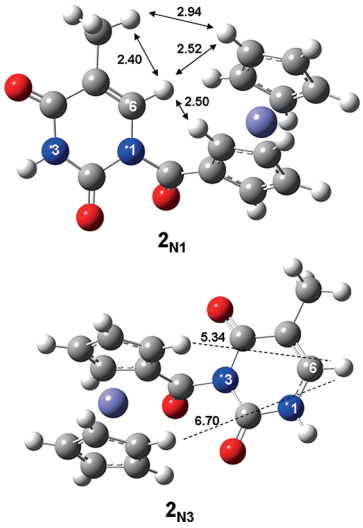

Figure 2. B3LYP/6-31G(d) optimized N^1- and N^3-substituted products ($\mathbf{2_{N1}}$ and $\mathbf{2_{N3}}$, resp.) of the reaction between thymine and ferrocenoyl chloride (FcCOCl). The double arrows indicate key ^{1}H-^{1}H NOESY correlations observed for $\mathbf{2_{N1}}$ (see the Supporting Information) and the corresponding interatomic distances [Å]. The dashed lines indicate the calculated distances [Å] between the 6-H atom and selected ferrocenyl protons in $\mathbf{2_{N3}}$.

The same conclusion comes from ^{19}F NMR spectroscopic measurements of the reaction between 5-fluorouracil and FcCOCl (the small inset in Figure 3). The peak at –178.3 ppm, which corresponds to deprotonated 5-fluorouracil, disappears in time, while a new signal at –166 ppm shows up as the only signal in the spectrum. Again, the detailed 2D NMR spectra (see below) confirmed that the product formed was the N^1-isomer ($\mathbf{2_{N1}}$, R = F).

Quantum chemical calculations have been employed to rationalize the preferential reaction of ferrocenoyl chloride with the N^1-nitrogen atom in uracil. At the B3LYP/6-31+G(d,p) level, the calculated Gibbs free energy of activation for the reaction at the N^3-position is approximately 40 kJ/mol higher than the barrier for the corresponding reaction at the N^1-position (Scheme 2 and Table 1).

The calculated energy of N^1-ferrocenyl-substituted uracil ($\mathbf{2_{N1}}$, R′ = Fc in Scheme 2) is similar to the energy of its N^3-substituted counterpart ($\mathbf{2_{N3}}$, R′ = Fc). Therefore, the N^1-acylation reaction $\mathbf{1_{N1}} \rightarrow \mathbf{2_{N1}}$ is not thermodynamically, but kinetically favored. The comparative computational study has been performed for the reaction between other acyl chlorides, benzoyl chloride (R′ = Ph) and acetyl chloride (R′ = Me), and other pyrimidine bases (thymine and 5-fluorouracil). In each case, the barrier for the N^1-reaction is lower than the corresponding barrier for the N^3-reaction (Table 1).

The results presented above confirm our hypothesis that regioselectivity in the reaction between the acylating agent (FcCOCl) and deprotonated pyrimidine nucleobases is kinetically controlled. Both reactions $\mathbf{1} \rightarrow \mathbf{2_{N1}}$ and $\mathbf{1} \rightarrow \mathbf{2_{N3}}$ (see Scheme 1, where R = H, Me, or F) are strongly exergonic (Table 1). The calculated Gibbs free energies (ΔG_r) for

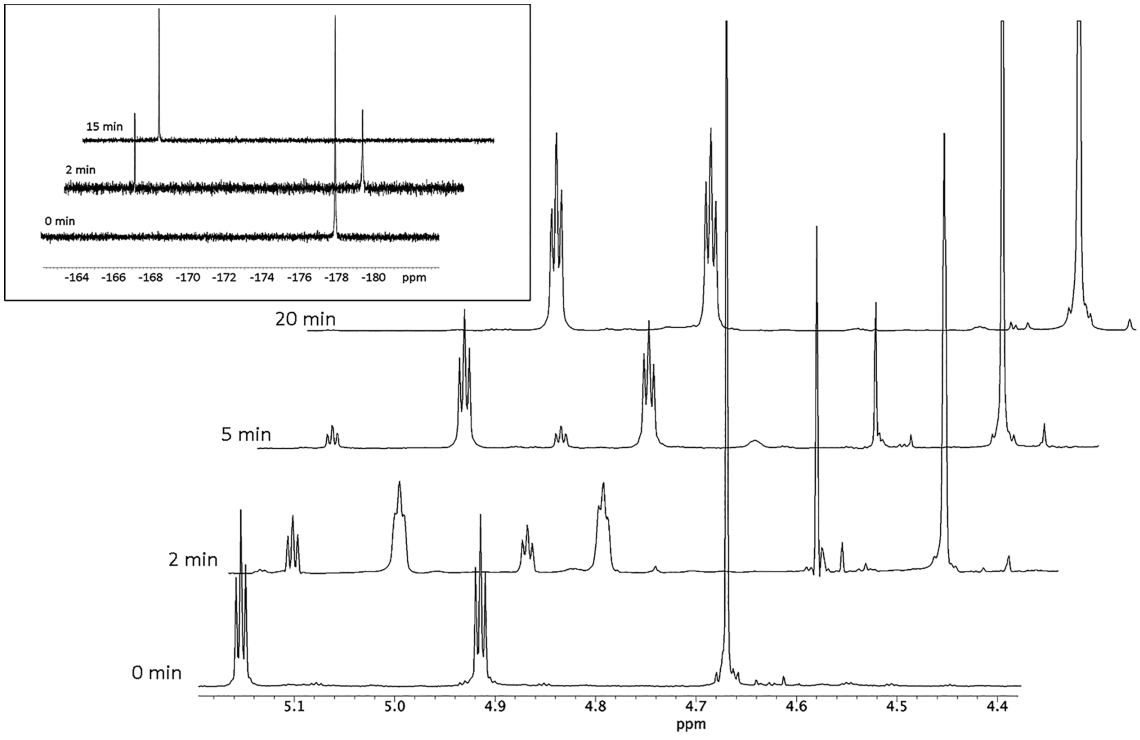

Figure 3. ^{1}H NMR (400 MHz) spectra (selected resonances) of the reaction mixture aliquots (thymine/NaH + FcCOCl in DMF) taken at several time points. The stack-plot of spectra (with an offset included) were recorded over 20 min. The small inset shows ^{19}F NMR (376 MHz) spectra of the reaction mixture (5-FU/NaH + FcCOCl in DMF) recorded over 15 min. All spectra were measured in [D_6]-DMSO at 25 °C.

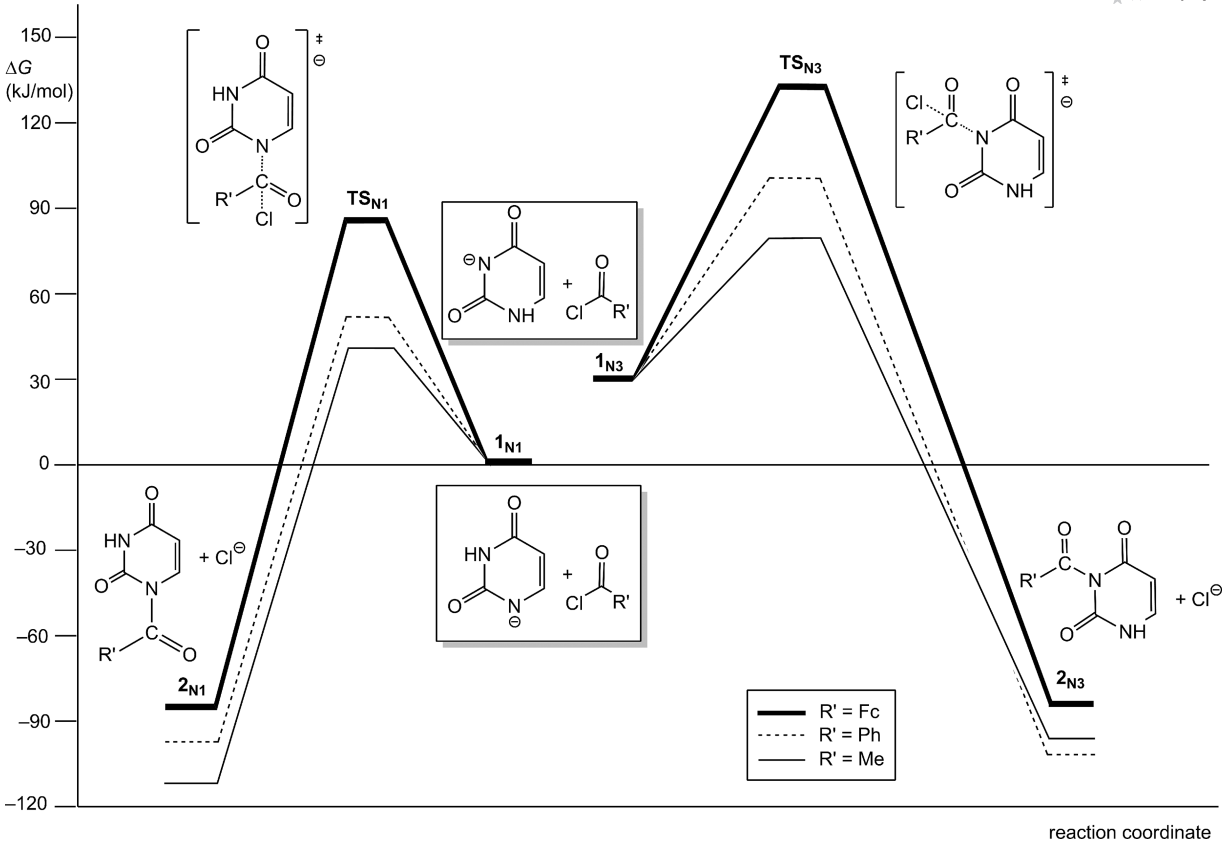

Scheme 2. Schematic energy profile [B3LYP/6-31+G(d,p) + ΔG_{solv}] for the reaction between deprotonated uracil (at N^1- or N^3-position) and a series of acylchlorides (R′ = Me, Ph, or Fc).

Table 1. Relative[a] Gibbs free energy of the reaction (ΔG_r) and activation barrier ($\Delta G^{\#}$) (in kJ/mol, at 298.15 K) for reactions between deprotonated nucleobases (at the N^1- or N^3-position) and acyl chlorides, calculated at the CPCM/UFF//B3LYP/6-31+G(d,p)/SDD level of theory.[b]

Acylation reaction at selected position		Uracil		Thymine		5-Fluorouracil	
		ΔG_r	$\Delta G^{\#}$	ΔG_r	$\Delta G^{\#}$	ΔG_r	$\Delta G^{\#}$
Base +	N^1	–116.4	39.4	–106.4	63.2	–89.3	75.5
MeCOCl	N^3	–95.1	78.3	–83.4	104.5	–65.4	93.3
Base +	N^1	–98.4	55.1	–84.0	80.3	–66.0	77.2
PhCOCl	N^3	–95.1	96.7	–86.2	124.5	–67.9	115.8
Base +	N^1	–84.3	87.8	–71.4	92.1	–53.4	97.6
FcCOCl	N^3	–83.6	134.9	–69.1	164.0	–50.9	153.9

[a] Sum of energies for the N^1-deprotonated base and acyl chloride is set to zero. [b] All geometries optimized at the B3LYP/6-31G(d) level, and bulk solvent effects have been calculated for DMF (ε = 37.22).

all reactions are between –50 and –120 kJ/mol. In each case, several product conformers are located (see the Supporting Information), and only the most stable are presented herewith (Table 1). In reactions between acetyl chloride and nucleobases the N^1-acetylated products are calculated as more stable (> 20 kJ/mol) than their N^3-counterparts. However, in reactions between benzoyl or ferrocenoyl chloride and nucleobases, the stability of N^1- and N^3-isomers is very similar. It comes out that the formation reactions of N^1- and N^3-ferrocenoylated products are almost isoenergetic processes ($\Delta\Delta G_r$ = 0.7 kJ/mol, for the reaction uracil + FcCOCl). This shows that the calculated thermochemical data, for parallel reactions at N^1- and N^3-positions, cannot explain the experimentally observed regioselectivity. As stated above, the regioselectivity of this reaction is mainly kinetically controlled.

NMR Analysis of the Reaction Mixture

The ^{13}C NMR spectra of previously reported acyl-substituted uracil and thymine reveal that N^1- and N^3-acylated derivatives can be distinguished on the basis of the chemical shifts of the corresponding C5 carbon resonance.[11] The C5 resonance signals of uracil and thymine are shifted approximately 3 ppm downfield with the introduction of the N^1-benzoyl substituent (Table 2). No such effect was observed with the introduction of the benzoyl group at the N^3-position.[11] In our case, the reaction between uracil/thymine and FcCOCl results in the ferrocenoylated product in which the C5 signal is also shifted approximately 3 ppm downfield compared with the corresponding signal of the parent nucleobases (Table 2). The introduction of the ferrocenoyl group, accompanied by the downfield shift of the C5 signal, is therefore indicative of N^1-substitution.

Table 2. Experimental[a] and computational [GIAO-CPCM/UFF//B3LYP/6-311G(d,p)//B3LYP/6-31G(d)/ Wachter-f method][b] NMR chemical shifts[c] for the C5 signal (and for the Fe atom, where appropriate) in pyrimidine bases and their N^1- and N^3-acylated derivatives (*Bz* = benzoyl, *Fc* = ferrocenoyl).

	C5 δ_{exp} (δ_{calc})	C5 $\Delta\delta_{exp}$ ($\Delta\delta_{calc}$)[d]	Fe δ_{calc}
Uracil	101.1 (101.8)	–	–
N^1-Bz-uracil	103.7 (105.0)	+2.6 (+3.2)	–
N^3-Bz-uracil	100.1 (102.2)	–1.0 (+0.4)	–
N^1-Fc-uracil	102.9 (104.0)	+1.8 (+2.2)	1970.4
N^3-Fc-uracil	n. a. (102.3)	n. a. (+0.5)	1984.8
Thymine	107.8 (111.6)	–	–
N^1-Bz-thymine	111.5 (115.4)	+3.7 (+3.8)	–
N^3-Bz-thymine	107.9 (112.2)	+0.1 (+0.6)	–
N^1-Fc-thymine	111.6 (114.6)	+3.8 (+3.0)	1919.0
N^3-Fc-thymine	n. a. (112.1)	n. a. (+0.5)	1935.8
5-Fluorouracil	139.9 (146.1)	–	–
N^1-Fc-5-fluorouracil	140.9 (147.2)	+1.0 (+1.1)	1935.5
N^3-Fc-5-fluorouracil	n. a. (145.9)	n. a. (–0.2)	1952.9

[a] Experimental NMR spectra measured in [D_6]DMSO. [b] Geometries were optimized and chemical shifts calculated in the model solvent [D_6]DMSO. [c] ^{13}C NMR chemical shifts are given in ppm downfield from tetramethysilane (TMS; 0 ppm), and ^{57}Fe NMR chemical shifts are relative to ferrocene (1532 ppm). [d] Difference between chemical shifts for C5 signals δ_{C5}(acylated base) – δ_{C5}(base).

To supplement the above experimental observation, we performed GIAO-NMR calculations for N^1- and N^3-acyl-substituted structures and for the parent pyrimidine bases (uracil and thymine). In agreement with experimental NMR spectroscopic data, a difference of 3.2 ppm was calculated (Table 2) for the C5 signal in uracil (δ_{calc} = 101.8 ppm) and in N^1-benzoyl-substituted uracil (δ_{calc} = 105.0 ppm). No significant difference between chemical shifts (C5 signal) was calculated in uracil and N^3-benzoyl-substituted uracil (δ_{calc} = 102.2 ppm). A similar result was found for thymine and its N^1- and N^3-benzoylated products (Table 2). This supports earlier claims that ^{13}C NMR spectroscopy can be a useful tool to differentiate N^1- vs. N^3-acylation products.

In the case of 5-fluorouracil, no significant chemical shift difference for the C5 signal in the parent 5-FU and N^1-ferrocenoyl-substituted 5-FU was observed either experimentally or theoretically. This is in line with the recent NMR study on 5-FU and its N^1-analogues.[16] However, according to NMR analysis of the reaction mixture (the small inset in Figure 3) we are confident that the regioselectivity in the reaction between 5-FU and FcCOCl follows the same pattern as that described for uracil and thymine.

Although the ^{57}Fe nucleus has a large chemical shift range[17] and ^{57}Fe NMR shift values can be very susceptible to slight changes in geometry;[18] we found less than 18 ppm relative difference between the calculated ^{57}Fe NMR chemical shifts in N^1- and N^3-ferrocenoylated nucleobases (Table 2). This suggests that ^{57}Fe NMR is probably not a sensitive tool to probe the preferred site of ferrocenoylation in pyrimidine bases.

In addition to downfield shifts observed for the C5 signal in N^1-acylated pyrimidine bases (ca. 3 ppm as compared with unsubstituted nucleobases), we found that ^1H-^1H NOESY correlations could also be a valuable tool to detect N^1-acylation products. In the case of N^1-ferrocenoyl-substituted thymine (**2_{N1}**, Figure 2), the NOESY experiment produces crosspeaks (see Figure S3 in the Supporting Information) between C6-H and ferrocenyl protons that are close in space (the calculated distances of ca. 2.5 Å). It is expected that no cross-relaxation between C6-H and ferrocenyl protons is possible in the N^3-isomer (**$2N^3$**, Figure 2), because the corresponding interatomic distances are larger than 5 Å. The same cross-polarization between C6-H and ferrocenyl protons is observed for uracil and 5-fluorouracil (see Figure S2 and S4 in the Supporting Information), which results in cross peaks in the corresponding 2D NOESY spectra. To conclude, a detailed analysis of both ^1H and ^{13}C NMR spectra reveals that N^1-ferrocenoylated products are formed preferentially in the reaction between the deprotonated pyrimidine nucleobase (using NaH as a deprotonating agent) and FcCOCl in dimethylformamide.

Conclusions

A facile and selective N^1-ferrocenoylation of pyrimidine nucleobases (uracil, thymine, and 5-fluorouracil) is reported. The synthetic procedure used to obtain only the N^1-regioisomer does not require any protection of the N^3-position in the nucleobase. Out of three deprotonating agents (K_2CO_3, TEA, and NaH), only sodium hydride appeared effective to assist the acetylation at the N^1-position.

1D and 2D NMR spectral evidence of regioselective N^1-ferrocenoylation of pyrimidine nucleobases has been presented. Reactions were followed by ^1H and ^{19}F NMR spectroscopy and only one product was detected. The structure and position of the substitution were confirmed by ^{13}C NMR spectroscopy. It is unambiguously identified as the N^1-regioisomer. We have shown that experimental NMR spectroscopic data analysis coupled with GIAO-NMR calculations is a valuable tool to differentiate between N^1- and N^3-acylated products.

The relative acidity of N^1–H vs. N^3–H bonds in nucleobases, the calculated thermochemical data of the reaction products (**2_{N1}** vs. **2_{N3}**), and energy barriers for the two parallel reactions, **$1 \rightarrow 2_{N1}$** vs. **$1 \rightarrow 2_{N3}$**, have been considered to explain the rationale behind the observed regioselectivity. It comes out that the regioselectivity is governed by kinetic factors only. The transition-state structures for N^1-ferrocenoylation of nucleobases (**TS_{N1}**) were calculated to be much more stable (> 40 kJ/mol) than the corresponding structures for N^3-ferrocenoylation (**TS_{N3}**) in each case.

According to our computational results at the CPCM/B3LYP/6-31+G(d,p)//B3LYP/6-31G(d) level of theory, the reaction between pyrimidine nucleobase and ferrocenoyl chloride follows a concerted S_N2-like mechanism. The nucleophilic attack of the deprotonated base on the carbonyl group of FcCOCl is a one-step process, which implies that no tetrahedral intermediate exists on the corresponding potential energy surface.

Computational Methods

Geometries were fully optimized at the B3LYP level of theory, as implemented in the Gaussian 09 software package.[19] The basis set for optimization was standard Pople's 6-31G(d) on non-metal atom centers, whereas the Stuttgart–Dresden–Bonn (SDD)[20] basis set with effective core potential (ECP) was used for Fe, similar to previous studies.[21] Improved, single-point energies were calculated at the B3LYP level with 6-31+G(d,p) basis set for non-metal centers, while SDD/ECP was used for Fe. This and comparable DFT levels have proven quite successful for transition-metal compounds and are well suited for the description of structures, energies, vibrational frequencies, and other properties.[22] Harmonic frequencies were computed from analytical second derivatives.

Gibbs energies of solvation were determined by using the CPCM continuum solvation model at the B3LYP/6-31+G(d,p)//B3LYP/6-31G(d) level, with the UFF atomic radii and electrostatic scaling factor (alpha value) set to 1.1 for all atoms (default values in Gaussian09).[23–25] The UFF cavities are selected to ensure that solvent spheres are placed around light and heavy atoms. The solvent relative permittivity of ε = 37.22 [*N*,*N*-dimethylformamide (DMF)] was used.

Magnetic shieldings (σ) were computed at the B3LYP level for the CPCM/B3LYP/6-31G(d) geometries optimized in dimethyl sulfoxide (DMSO, ε = 46.83), employing GIAOs (gauge including atomic orbitals)[26] with the augmented Wachters basis[27] on Fe (8s7p4d), and 6-311G(d,p) basis on all other atoms. Chemical shifts were calculated relative to tetramethylsilane (TMS; ^{13}C and ^{1}H magnetic shieldings are 181.29 and 31.86 at the same level) or ferrocene (^{57}Fe, ^{13}C, and ^{1}H magnetic shieldings are –5299.35, 110.33, and 28.11), using the experimental $\delta(^{57}\text{Fe})$ value of ferrocene (1532 ppm).[28] All NMR shieldings were Boltzmann-averaged by selection of the most stable conformers (see the Supporting Information).

IRC calculations (intrinsic reaction coordinate as implemented in Gaussian 09) were performed at the corresponding level to identify the minima connected through the transition state. The initial geometries used were that of the corresponding transition structures, and the paths were followed in both directions from that point. This method verified that a given transition state structure indeed connected the presumed energy minimum structures.[29]

To account for the entropic effect of the presence of solvent molecules around a solute, the cell model presented by Ardura et al. was used.[30] This model is proposed in order to explicitly evaluate the effect of the loss of translation degrees of freedom in solution on the Gibbs activation energy in bimolecular (or higher order of molecularity) reactions. It has been shown that the standard implementation of the continuum model is not capable of adequately estimating the increase in Gibbs energy corresponding to the constriction of the translation motion of the species along the reaction coordinate when passing from the gas phase to the solution. According to the cell model, the difference $\Delta\Delta G_{sol}$ between the two Gibbs energy variations $\Delta G^{\#}_{sol}$ and ΔG_{sol} for bimolecular reaction A + B→A–B is:

$$\Delta\Delta G_{sol} = \Delta G^{\#}_{sol} - \Delta G_{sol} = RT\ln[(v_c(A)v_c(B)/v_c(A\text{-}B)] - RT\ln[k_B T/p]$$

where v_c corresponds to the cavity volume, and k_B, T, and p, correspond to the Boltzmann constant, temperature, and pressure, respectively. The cavity volume for each species was obtained from CPCM calculation.

Experimental Section

Methods and Materials: The syntheses were carried out under an argon atmosphere in anhydrous solvents. Melting points were determined with a Büchi apparatus. The IR spectra were recorded for KBr pellets or CH_2Cl_2 solutions with a Bomem MB100 Mid FT IR spectrophotometer. The mass spectra were acquired with a 4800 MALDI TOF/TOF-MS Analyzer. The ^{1}H, ^{13}C, and ^{19}F NMR spectra of [D_6]DMSO or $CDCl_3$ solutions were recorded with a Varian INOVA 400 spectrometer. The spectrometer operated at 399.6 MHz (^{1}H), 375.9 MHz (^{19}F), and 100.5 MHz (^{13}C). Chemical shifts in the ^{1}H NMR and ^{13}C NMR spectra are expressed in parts per million (ppm) vs. TMS as the external standard, and ^{19}F chemical shifts are referenced to $CFCl_3$ as the external standard.

Products were purified by column chromatography (Fluka, silica gel, 90 Å, 70–230 mesh) using the CH_2Cl_2/acetone mixtures (10:1). *N*,*N*-Diphenylferrocenecarboxamide was prepared in 54% yield starting from ferrocene and *N*,*N*-diphenylcarbamoyl chloride.[31] Alkaline hydrolysis of *N*,*N*-diphenylcarbamoyl chloride gave ferrocenecarboxylic acid in 80%.[32]

Synthesis of Ferrocenoyl Chloride: To a suspension of ferrocenecarboxylic acid (300 mg, 1.3 mmol) and freshly distilled oxalyl chloride (274 mL, 3.13 mmol) in anhydrous CH_2Cl_2 (5 mL), one drop of pyridine was added. The reaction mixture was heated to reflux for 2 h and the solvents were evaporated in vacuo to dryness to give a dark residue. The crude product was repeatedly extracted at 80 °C for 10 min with petroleum ether to give red FcCOCl crystals (275 mg, 85%).[33] IR (CH_2Cl_2): $\tilde{\nu}$ = 2958 (w, C–H, Fc), 1755 (s, C=O) cm^{-1}. ^{1}H NMR (400 MHz, $CDCl_3$, 25 °C): δ = 4.9 (t, $^{3}J_{H,H}$ = 1.9 Hz, 2 H, H-α′), 4.6 (t, $^{3}J_{H,H}$ = 1.9 Hz, 2 H, H-β′), 4.4 (s, 5 H, Cp) ppm. ^{13}C NMR (100 MHz, $CDCl_3$, 25 °C): δ = 178.3 (CO), 73.3 (Ci), 71.7 (Cp), 71.2 (C-β′), 70.4 (C-α′) ppm.

Synthesis of Ferrocenoyl Ethyl Carbonate: A suspension of ferrocenecarboxylic acid (500 mg, 2.175 mmol) in water (0.41 mL) was dissolved by the addition of acetone (7.4 mL) and then cooled to 0 °C. Triethylamine (7.4 μL) in acetone (4.5 mL) is added dropwise, followed by the addition of ethyl chloroformate (5.8 μL) in acetone (1.15 mL). After stirring for 30 min, the reaction mixture was evaporated, and the ferrocenoyl ethyl carbonate crude product (orange solid) was used for reactions with pyrimidine bases. IR (CH_2Cl_2): $\tilde{\nu}$ = 2932 (w, C–H, Fc), 1770 (s, C=O), 1713 (s, C=O), 1675 (s, C=O), 1047 (s, C–O) cm^{-1}. ^{1}H NMR (400 MHz, $CDCl_3$, 25 °C): δ = 4.9 (t, $^{3}J_{H,H}$ = 1.8 Hz, 2 H, H-α′), 4.6 (t, $^{3}J_{H,H}$ = 1.8 Hz, 2 H, H-β′), 4.4 (s, 5 H, Cp), 4.3 (q, $^{3}J_{H,H}$ = 7.2 Hz, 2 H, CH_2), 1.4 (t, $^{3}J_{H,H}$ = 7.2 Hz, 3 H, CH_3) ppm. ^{13}C NMR (100 MHz, $CDCl_3$, 25 °C): δ = 167.7 (FcCO), 161.8 (CO), 72.7 (C-α′), 70.8 (C-β′), 70.2 (Cp), 69.3 (Ci), 61.2 (CH_2), 14.3 (CH_3) ppm.

General Procedure for the Preparation of N^{1}-Ferrocenoylated Pyrimidine Bases: Sodium hydride (NaH; 1.5 mmol), was added portionwise to pyrimidine bases (1 mmol) suspended in DMF (3 mL). After stirring at room temperature for 30 min, FcCOCl (1 mmol) (or

FcCOOCOOEt in selected cases) was added dropwise to the clear solution. The mixture was stirred for 10–30 min and then neutralized with 10% aqueous solution of citric acid and extracted with CH_2Cl_2. The organic layer was washed with water and the solvents were evaporated under vacuum. Subsequent purification by column chromatography afforded N^1-ferrocenoylated pyrimidine bases.

N^1-Ferrocenoyluracil (2_{N1}, R = H): Red-orange crystals (269.6 mg, 64.6% yield); m.p. > 200 °C. $C_{15}H_{12}FeN_2O_3$ (324.112): calcd. C 55.59, H 3.73, O 14.81, N 8.64; found C 55.61, H 3.75, O 14.84, N 8.67. IR (CH_2Cl_2): $\tilde{\nu}$ = 3374 (w, NH), 3099 (w, CH, Fc), 1700 (s, C=O), 1633 (w, C=O) cm^{-1}. ^1H NMR (400 MHz, [D$_6$]DMSO, 25 °C): δ = 11.5 (s, 1 H, N^3-H), 8.0 (d, $^3J_{H,H}$ = 8.0 Hz, 1 H, C6-H), 5.7 (d, $^3J_{H,H}$ = 8.0 Hz, 1 H, C5-H), 4.9 (t, $^3J_{H,H}$ = 2.0 Hz, 2 H, H-β′), 4.7 (t, $^3J_{H,H}$ = 2.0 Hz, 2 H, H-α′), 4.3 (s, 5 H, Cp) ppm. ^{13}C NMR (100 MHz, [D$_6$]DMSO, 25 °C): δ = 173.6 (FcCO), 163.8 (C4), 149.9 (C2), 141.3 (C6), 102.9 (C5), 74.1 (C-α′), 72.6 (Ci), 71.9 (C-β′), 71.1 (Cp) ppm. HRMS (MALDI-TOF/TOF): *m*/*z* calcd. for $C_{15}H_{12}O_3N_2Fe$ $[M + H]^+$ 325.1203; found 325.1205.

N^1-Ferrocenoylthymine (2_{N1}, R = Me): Orange crystals (245.79 mg, 72.7% yield); m.p. > 200 °C. $C_{16}H_{14}FeN_2O_3$ (338.139): calcd. C 56.83, H 4.17, O 14.19, N 8.28; found C 56.85, H 4.18, O 14.21, N 8.29. IR (CH_2Cl_2): $\tilde{\nu}$ = 3375 (w, NH), 2927 (w, CH, Fc), 1730 (s, C=O), 1700 (s, C=O) cm^{-1}. ^1H NMR (400 MHz, [D$_6$]DMSO, 25 °C): δ = 11.5 (s, 1 H, N^3-H), 7.9 (q, $^4J_{H,H}$ = 1.3 Hz, 1 H, C6-H), 4.8 (t, $^3J_{H,H}$ = 2.2 Hz, 2 H, H-α′), 4.7 (t, $^3J_{H,H}$ = 2.2 Hz, 2 H, H-β′), 4.3 (s, 5 H, Cp), 1.8 (d, $^4J_{H,H}$ = 1.3 Hz, 3 H, CH_3) ppm. ^{13}C NMR (100 MHz, [D$_6$]DMSO, 25 °C): δ = 173.7 (FcCO), 164.6 (C4), 149.9 (C2), 136.6 (C6), 111.6 (C5), 73.8 (C-α′), 72.9 (Ci), 71.9 (C-β′), 71.1 (Cp), 12.3 (CH_3) ppm. HRMS (MALDI-TOF/TOF): *m*/*z* calcd. for $C_{16}H_{14}O_3N_2Fe$ $[M + H]^+$ 339.1469; found 339.1470.

N^1-Ferrocenoyl 5-Fluorouracil (2_{N1}, R = F): Purple crystals (203.04 mg, 59.4% yield); m.p. > 200 °C. $C_{15}H_{11}FFeN_2O_3$ (342.108): calcd. C 52.66, H 3.24, O 14.03, N 8.19; found C 52.62, H 3.22, O 14.00, N 8.16. IR (CH_2Cl_2): $\tilde{\nu}$ = 3366 (w, NH), 2924 (w, C–H, Fc), 1720 (s, C=O), 1648 (s, C=O) cm^{-1}. ^1H NMR (400 MHz, [D$_6$]DMSO, 25 °C): δ = 12.0 (s, 1 H, N^3-H), 8.4 (d, $^3J_{F,H}$ = 6.4 Hz, 1 H, C6-H), 4.9 (t, $^3J_{H,H}$ = 2.3 Hz, 2 H, H-α′), 4.7 (t, $^3J_{H,H}$ = 2.3 Hz, 2 H, H-β′), 4.3 (s, 5 H, Cp) ppm. ^{13}C NMR (100 MHz, [D$_6$]DMSO, 25 °C): δ = 172.7 (FcCO), 158.1 (d, $^3J_{F,C}$ = 27.1 Hz, C4), 148.6 (C2), 140.9 (d, $^2J_{F,C}$ = 234.5 Hz, C5), 125.7 (d, $^3J_{F,C}$ = 36.1 Hz, C6), 73.9 (C-α′), 72.5 (Ci), 71.9 (C-β′), 71.1 (Cp) ppm. ^{19}F NMR (376 MHz, [D$_6$]DMSO, 25 °C): δ = –167.4 (d, $^3J_{H,F}$ = 6.4 Hz, C5-F) ppm. HRMS (MALDI-TOF/TOF): *m*/*z* calcd. for $C_{15}H_{11}FO_3N_2Fe$ $[M + H]^+$ 343.1108; found 343.1111.

Supporting Information (see footnote on the first page of this article): Cartesian coordinates and calculated energies for all computed structures and additional NMR spectroscopic data for products.

Acknowledgments

The research was supported by the University of Zagreb (grant number KFPI 1.1.1.8). The authors thank the Computing Centre SRCE for allocating computer time on the Isabella cluster. The authors thank Professor Branka Zorc for the generous donation of selected chemicals, and Ivana Amerl for the technical assistance. The NMR instrument donation from Symrise AG is gratefully acknowledged.

[1] a) V. Sai Sudhir, C. Venkateswarlu, O. T. Muhammed Musthafa, S. Sampath, S. Chandrasekaran, *Eur. J. Org. Chem.* **2009**, 2120–2129; b) G. Mwande-Maguene, J. Jakhal, J.-B. Lekana-Douki, E. Mouray, T. Bousquet, S. Pellegrini, P. Grellier, F. S. T. Ndouo, J. Lebibi, L. Pelinski, *New J. Chem.* **2011**, *35*, 2412–2415; c) S. I. Kirin, H.-B. Kraatz, N. Metzler-Nolte, *Chem. Soc. Rev.* **2006**, *35*, 348–354; d) M. Patra, G. Gasser, M. Wenzel, K. Merz, J. E. Bandow, N. Metzler-Nolte, *Organometallics* **2010**, *29*, 4312–4319; e) J. Lapić, S. Djaković, I. Kodrin, Z. Mihalić, M. Cetina, V. Rapić, *Eur. J. Org. Chem.* **2010**, 2512–2524; f) B. Adhikari, R. Afrasiabi, H.-B. Kraatz, *Organometallics* **2013**, *32*, 5899–5905; g) H.-B. Kraatz, *J. Inorg. Organomet. Polym.* **2005**, *15*, 83–106; h) T. Moriuchi, T. Hirao, *Acc. Chem. Res.* **2010**, *43*, 1040–1051.

[2] a) A. N. Patwa, R. G. Gonnade, V. A. Kumar, M. M. Bhadbhade, K. N. Ganesh, *J. Org. Chem.* **2010**, *75*, 8705–8708; b) H. V. Nguyen, A. Sallustrau, J. Balzarini, M. R. Bedford, J. C. Eden, N. Georgousi, N. J. Hodges, J. Kedge, Y. Mehellou, C. Tselepis, J. H. R. Tucker, *J. Med. Chem.* **2014**, *57*, 5817–5822; c) A. A. Simenel, G. A. Dokuchaeva, L. V. Snegur, A. N. Rodionov, M. M. Ilyin, S. I. Zykova, L. A. Ostrovskaya, N. V. Bluchterova, M. M. Fomina, V. A. Rikova, *Appl. Organomet. Chem.* **2011**, *25*, 70–75; d) H. V. Nguyen, Z. Zhao, A. Sallustrau, S. L. Horswell, L. Male, A. Mulas, J. H. R. Tucker, *Chem. Commun.* **2012**, *48*, 12165–12167; e) K. Kowalski, J. Skiba, L. Oehninger, I. Ott, J. Solecka, A. Rajnisz, B. Therrien, *Organometallics* **2013**, *32*, 5766–5773; f) A. Houlton, C. J. Isaac, A. E. Gibson, B. R. Horrocks, W. Clegg, M. R. J. Elsegood, *J. Chem. Soc., Dalton Trans.* **1999**, 3229–3234; g) P. Brázdilová, M. Vrábel, R. Pohl, H. Pivoňková, L. Havran, M. Hocek, M. Fojta, *Chem. Eur. J.* **2007**, *13*, 9527–9533.

[3] D. B. Longley, D. P. Harkin, P. G. Johnston, *Nature Rev.* **2003**, *3*, 330–338.

[4] M. A. Kurinovich, J. K. Lee, *J. Am. Chem. Soc.* **2000**, *122*, 6258–6262.

[5] A. Zhachkina, J. K. Lee, *J. Am. Chem. Soc.* **2009**, *131*, 18376–18385.

[6] V. Verdolino, R. Cammi, B. H. Munk, H. B. Schlegel, *J. Phys. Chem. B* **2008**, *112*, 16860–16873.

[7] J. M. Fox, O. Dmitrenko, L. Liao, R. D. Bach, *J. Org. Chem.* **2004**, *69*, 7317–7328.

[8] T. W. Bentley, G. Llewellyn, J. A. McAlister, *J. Org. Chem.* **1996**, *61*, 7927–7932.

[9] F. Ruff, O. Farkas, *J. Phys. Org. Chem.* **2011**, *24*, 480–491.

[10] J. March, in: *Advanced Organic Chemistry*, 4th ed.; Wiley: New York, **1992**, p. 330–335.

[11] K. A. Cruickshank, J. Jiricny, C. B. Reese, *Tetrahedron Lett.* **1984**, *25*, 681–684.

[12] M. N. S. Rad, S. Behrouz, Z. Asrari, A. Khalafi-Nezhad, *Monatsh. Chem.* **2014**, *145*, 1933–1940.

[13] S. A. Lahsasni, *Nucleosides Nucleotides Nucleic Acids* **2013**, *32*, 439–452.

[14] T. Kametani, K. Kigasawa, M. Hiiragi, K. Wakisaka, S. Haga, Y. Nagamatsu, H. Sugi, K. Fukawa, O. Irino, *J. Med. Chem.* **1980**, *23*, 1324–1329.

[15] A. Nováček, I. Hedrlín, *Collect. Czech. Chem. Commun.* **1967**, *32*, 1045–1050.

[16] G. S. Abdrakhimova, M. Y. Ovchinnikov, A. N. Lobov, L. V. Spirikhin, S. P. Ivanov, S. L. Khursan, *J. Phys. Org. Chem.* **2014**, *27*, 876–883.

[17] P. S. Pregosin, in: *Transition Metal Nuclear Magnetic Resonance* (Ed.: P. S. Pregosin), Elsevier, Amsterdam, **1991**.

[18] a) M. Bühl, F. T. Mauschick, F. Terstegen, B. Wrackmeyer, *Angew. Chem. Int. Ed.* **2002**, *41*, 2312–2315; *Angew. Chem.* **2002**, *114*, 2417; b) B. Wrackmeyer, O. L. Tok, A. Ayazi, H. E. Maisel, M. Herberhold, *Magn. Reson. Chem.* **2004**, *42*, 827–830; c) A. Šarić, V. Vrček, M. Bühl, *Organometallics* **2008**, *27*, 394–401; d) J. Lapić, M. Cetina, D. Šakić, S. Djaković, V. Vrček, V. Rapić, *ARKIVOC* **2010**, *9*, 257–268.

[19] M. J. Frisch, G. W. Trucks, H. B. Schlegel, G. E. Scuseria, M. A. Robb, J. R. Cheeseman, G. Scalmani, V. Barone, B. Mennucci, G. A. Petersson, H. Nakatsuji, M. Caricato, X. Li, H. P. Hratchian, A. F. Izmaylov, J. Bloino, G. Zheng, J. L. Son-

nenberg, M. Hada, M. Ehara, K. Toyota, R. Fukuda, J. Hasegawa, M. Ishida, T. Nakajima, Y. Honda, O. Kitao, H. Nakai, T. Vreven, J. A. Montgomery Jr., J. E. Peralta, F. Ogliaro, M. Bearpark, J. J. Heyd, E. Brothers, K. N. Kudin, V. N. Staroverov, R. Kobayashi, J. Normand, K. Raghavachari, A. Rendell, J. C. Burant, S. S. Iyengar, J. Tomasi, M. Cossi, N. Rega, J. M. Millam, M. Klene, J. E. Knox, J. B. Cross, V. Bakken, C. Adamo, J. Jaramillo, R. Gomperts, R. E. Stratmann, O. Yazyev, A. J. Austin, R. Cammi, C. Pomelli, J. W. Ochterski, R. L. Martin, K. Morokuma, V. G. Zakrzewski, G. A. Voth, P. Salvador, J. J. Dannenberg, S. Dapprich, A. D. Daniels, O. Farkas, J. B. Foresman, J. V. Ortiz, J. Cioslowski, D. J. Fox, *Gaussian 09*, revision D.01, Gaussian, Inc., Wallingford CT, **2009**.

[20] M. Dolg, U. Wedig, H. Stoll, H. Preuß, *J. Chem. Phys.* **1987**, *86*, 866–872.

[21] a) T. Romero, A. Caballero, A. Espinosa, A. Tárraga, P. Molina, *Dalton Trans.* **2009**, 2121–2129; b) W.-Y. Wang, N.-N. Ma, S.-L. Sun, Y.-Q. Qiu, *Phys. Chem. Chem. Phys.* **2014**, *16*, 4900–4910.

[22] W. Koch, M. C. Holthausen, in: *A Chemist's Guide to Density Functional Theory*; Wiley-VCH, Weinheim, Germany, **2000**, and the extensive bibliography therein.

[23] M. Cossi, G. Scalmani, N. Rega, V. Barone, *J. Chem. Phys.* **2002**, *117*, 43–54.

[24] V. Barone, M. Cossi, J. Tomasi, *J. Chem. Phys.* **1997**, *107*, 3210–3221.

[25] V. Barone, M. Cossi, *J. Phys. Chem. A* **1998**, *102*, 1995–2001.

[26] J. R. Cheeseman, G. W. Trucks, T. A. Keith, M. J. Frisch, *J. Chem. Phys.* **1996**, *104*, 5497–5509.

[27] a) A. J. H. Wachters, *J. Chem. Phys.* **1970**, *52*, 1033–1036; b) P. J. Hay, *J. Chem. Phys.* **1977**, *66*, 4377–4384.

[28] E. Haslinger, W. Robin, K. Schloegel, W. Weissensteiner, *J. Organomet. Chem.* **1981**, *218*, C11.

[29] C. Gonzales, H. B. Schlegel, *J. Phys. Chem.* **1990**, *4*, 5523–5527.

[30] D. Ardura, R. López, T. L. Sordo, *J. Phys. Chem. B* **2005**, *109*, 23618–23623.

[31] a) W. F. Little, R. Eisenthal, *J. Am. Chem. Soc.* **1960**, *82*, 577–580; b) J. Lapić, A. Pezerović, M. Cetina, S. Djaković, V. Rapić, *J. Mol. Struct.* **2011**, *990*, 209–216.

[32] A. Sonoda, I. Moritani, *J. Organomet. Chem.* **1971**, *26*, 133–140.

[33] H. J. Lorkowski, R. Pannier, A. Wende, *J. Prakt. Chem.* **1967**, *35*, 149–158.

Received: May 19, 2015
Published Online: July 17, 2015

